

A Sustainable Concept for Permafrost Thermal Stabilization

Egor Y. Loktionov^{a,*}, Elizaveta S. Sharaborova^a, Taissia V. Shepitko^b

^a Bauman Moscow State Technical University, 5-1, 2nd Baumanskaya str., Moscow 105005, Russia

^b Russian University of Transport, 9b9, Obraztsova str., Moscow 127994, Russia

Abstract

Although permafrost thermal stabilization systems have been used for a long time already, they have always had shortcomings and limitations of performance which has become even more pronounced in the warming climate. Those could be overcome to some extent, but at high cost mainly defined by need in energy supply. We have suggested a novel concept combining improved energy efficiency and solar power to ensure significant reduction of the thawing layer (to 20 cm order). We have performed calculations for the broad range of permafrost conditions to compare traditional methods for thermal stabilization and their combination to the suggested concept. The latter only has ensured minimum thawing layer over summer even at the southern edge of permafrost extent. The importance of minimum thawing layer is discussed in terms of chemical and biological safety in the area of human activities. The layout for glaciers protection has also been considered. Estimated cost of the concept implementation (ca. 180 \$/m²) is just slightly higher than for widely used thermosyphons while providing much better performance.

Keywords: solar energy; heat pumps; thermal state control; thawing; climate change.

1. Introduction

Permafrost is considered to be a part of the upper crustal layer, characterized by a subzero temperature of rocks and / or soil for two or more years and the absence of seasonal thawing. Permafrost underlies 24% of land surface in Northern Hemisphere (about 22.8 million km²),

* corresponding author: yagor@bmstu.ru, +7 903 786 9566

27 including more than 11 million km² in Russia, giving ca. 65% of the country's territory [1]. The
28 general trend for global temperature increase leads to permafrost thawing.

29 Global warming is currently most pronounced in the Arctic, leading to up to
30 0.075°C/year air and 0.1°C/year soil temperature increase [2-4]. In the near future, soil surface
31 temperature within the permafrost areas is going to increase by up to 2.3°C, leading to thawed
32 layer depth increase by 33% and permafrost region edge shift by 50–600 km north [5].
33 Permafrost thawing is normally accelerated under constructions leading to deformations [6], and
34 now it starts to cause disasters, e.g., recent 20 000 t diesel fuel spill in Norilsk, Russia [7]. This
35 problem becomes very urgent in Russia, and cost-effective measures to prevent the destruction
36 of structures located in permafrost areas need to be developed. Thawing also happens to glaciers,
37 so extraordinary measures are implemented to stop this process at some sites [8], in part, to
38 prevent disasters that could be easily induced at metastable balance interruption, e.g., by an
39 earthquake.

40 Construction on permafrost soil has always been full of challenges [9]. Most were
41 resolved at reasonable cost, to large extent, using thermosyphons for enhanced soil freezing
42 during winter time so it is not considerably thawed during summer [10]. Now, the cost of
43 sufficient solutions increases drastically, as well as need for constant monitoring of constructions
44 state. This problem becomes particularly pronounced for linear infrastructural objects such as
45 motorways [11], railroads [12], pipe [10] and power [13] lines connecting sparse settlements
46 across the wilderness. To prevent disasters, chilling units accompanied by power plants, fuel
47 tanks, and staff have to be brought in the most critical cases.

48 Basically, permafrost thawing happens as winters become milder and shorter while
49 summers become hotter and longer. Particularly for this reason, widely used thermosyphons are
50 currently operated out of designed conditions, so are not capable of keeping soil frozen. Heat is
51 supplied to soil via convection at natural air motion, solar radiation absorption, and also comes
52 with liquid precipitation. There are solutions to minimize this heat flow: solar reflectors and

53 shields [14], heat insulation [12] and waterproof layers [11]. Even such an exotic way as grazing
54 livestock is considered to suppress snow accumulation, and so getting better soil freezing in
55 winter [15]. But obviously neither of these passive methods is capable of complete ambient heat
56 rejection. Active cooling methods are well developed in general, but demand power supply, so
57 are very expensive. However, sufficient energy could be obtained at right-of-way land of linear
58 infrastructure objects using solar power plants [16]. Recently, suggestions to use solar powered
59 devices for thermal stabilization of permafrost railroads embankments have appeared [17, 18].

60 Preliminary results showing potential capability of keeping soil frozen using local
61 resources have been published earlier [17]. In this article, we are presenting more detailed
62 calculations results at different climatic conditions and discuss possible technical layouts for a
63 sustainable thermal stabilization system.

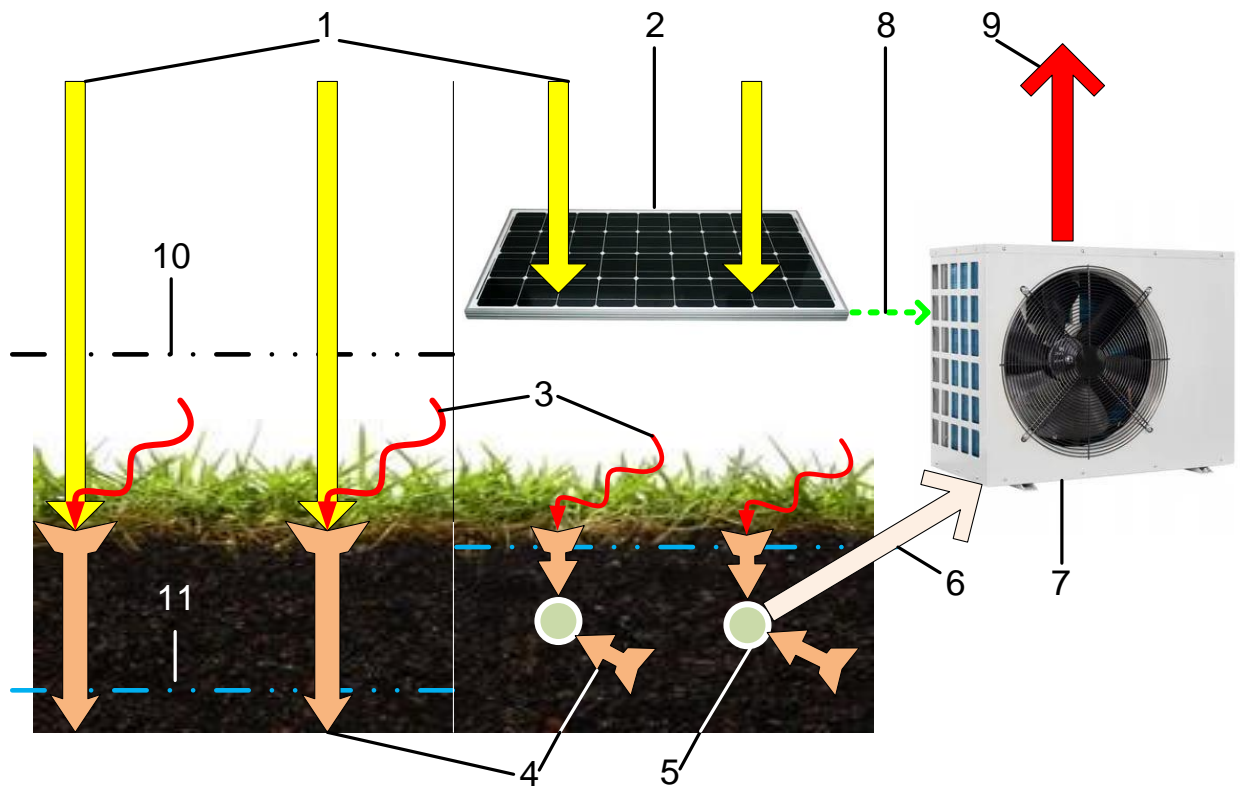
64

65 **2. Theory**

66 The main idea of our concept is to make solar radiation cool rather than heat the soil, for this:

- 67 1) soil has to be shielded from solar radiation and precipitation to the maximum extent,
68 since the snow does not reach the ground either, it is better frozen in winter, and
69 convection in summer is also partially suppressed;
- 70 2) better than just shielded, solar energy should be converted to electricity using
71 photovoltaics (PV), thermovoltaics or their combination as well as collected in thermal
72 form using vacuum pipes or plate collectors to drive the chiller;
- 73 3) regardless of which cooling principle is used (vapor compression [18], magnetocaloric
74 [19], sorption [20]), the devices use either electricity or both electricity and heat obtained
75 at previous step;
- 76 4) cooled near-surface layer should be organized to make a barrier for ambient heat
77 penetration in depth rather than cooling huge volumes of soil as with thermosyphons, for
78 that, probes are placed parallel to the ground surface within the natural thawing layer.

79 The general layout for this concept implementation is presented in Figure 1. All needed
 80 technologies are well developed and just need to be combined in the most efficient way. Thermal
 81 inertia of the soil makes the inconvenience associated with the intermittent power supply from
 82 renewable energy sources negligible.



83
 84 Figure 1. General schematic of a concept (right) compared to natural conditions (left): 1 – solar
 85 radiation; 2 – solar energy converter; 3 – convective heat flux; 4 – conductive heat flux; 5 –
 86 ground probes; 6 – heat sink from ground probes; 7 – chiller; 8 – converted solar energy; 9 –
 87 resulting heat sink; 10 – snow cover height; 11 – thawing layer.

88

89

90 3. Calculations

91 Using QGIS v.2.18 open software, we have developed a geographic information system
 92 (GIS) containing layers (Figure 2) with data for: solar irradiation (global (GHI) and direct (DHI)
 93 on horizontal surface, monthly, annual) [21], air temperature (monthly) [21-23], wind speed
 94 (monthly) [21], soil temperature (different depths, monthly) [23], permafrost extension (by

95 types) [24], railroads (by electrification type). Using these data, we have picked three test sites
96 with rather different conditions: Norilsk (N 69.33°, E 88.21°), Yakutsk (N 62.03°, E 129.74°),
97 and Chita (N 52.03°, E 113.5°). The former two are close to the terminal stations, and new
98 railroads are going to be built there soon across continuous and slightly discontinuous
99 permafrost. The latter is at the intensely used Trans-Siberian railroad, where traffic limitations
100 occur due to the discontinuous and sporadic permafrost thawing. Since Melnikov Permafrost
101 Institute of the Russian Academy of Sciences is located in Yakutsk, the most detailed data exist
102 for this site; so it was used for most tests and preliminary evaluations.

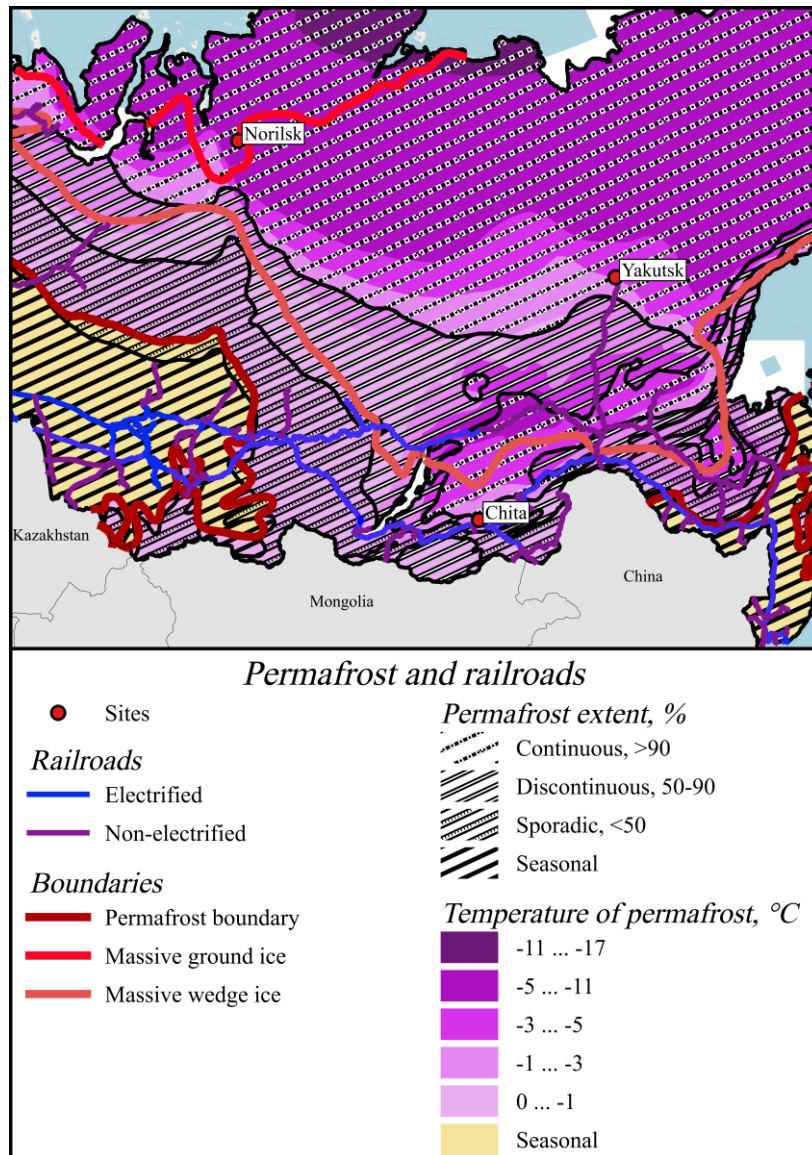
103 For thermal calculations, we have used Frost-3D Multi-Core GPU software
104 (<https://frost3d.ru/eng/>) which has been specially developed for permafrost soil calculations, its
105 results validity has been verified by analytical solutions [25] and practical applications,
106 compared to the most popular FEM packages [26], and conformity to relevant national and
107 corporate (Gazprom) construction regulations certified. We realize more accurate (and inevitably
108 more complicated) calculation methods might exist, but our aim at this stage was not to evaluate
109 temperature distributions precisely, but to see if our concept is viable and to what extent.

110 The calculation area and soil properties are presented in Figure 3 and Table 1. Time
111 increment of 1 month was taken. Under solar shields, solar radiation was taken as 0.05 of GHI,
112 wind speed as 0.3 of nominal (at 10 m). September 2015 was taken as a start point for
113 calculations opposed to January, to have soil unfrozen. Temperature distribution graphs are
114 provided for the embankment axis.

115 Initially, we have calculated temperature distributions for 5 years at natural conditions to
116 see whether heat fluxes are balanced. In case misbalance was observed, we adjusted soil layers
117 composition since there are no precise data for this parameter for the exact soil temperature
118 reference site. Then we have considered cases with sun shields, heat insulation, thermosyphons,
119 sun shields + ground probes, sun shield + thermosyphons presence all applied to the North–

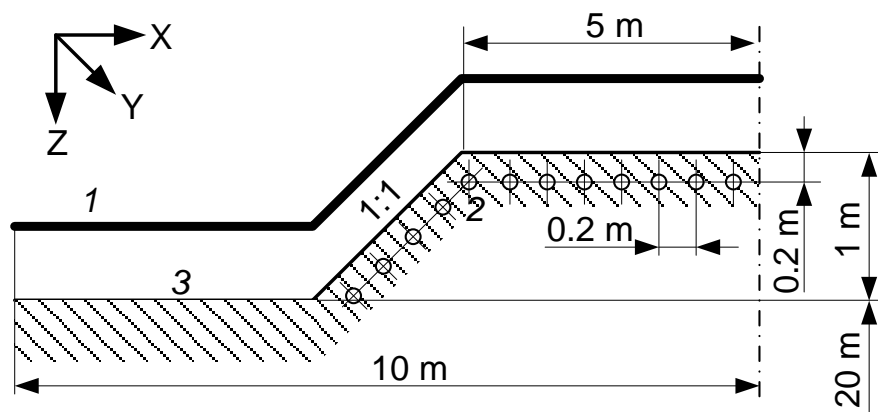
120 South railroad embankment. Calculations were performed for 5 subsequent years to see when the
121 new equilibrium state is reached.

122 We have considered the case of vapor compression heat pump powered by PV as the
123 easiest to implement on site. Electric power capacity was evaluated using GHI and PV
124 conversion efficiency of 10% (intentionally taken lower than most commercial products state for
125 standard test conditions (STC)). Heat pump cooling capacity was evaluated by multiplication of
126 the electric power capacity by COP, dependent on ambient air temperature t_a ($^{\circ}\text{C}$) as $\text{COP} =$
127 $4.8 - 0.12t_a$. For calculations, it affected heat exchange rate α inside the ground probes to match
128 the available cooling capacity. Mid summer drop in COP was compensated to some extent by
129 higher solar irradiation, and average α was $45.7 \text{ W}/(\text{m}^2\text{K})$. These figures are reached for PV
130 power achieved from the same area where ground probes are placed (the embankment). In our
131 calculation area (Figure 3), solar panels are placed outside the embankment too, providing extra
132 shielding to the soil and energy for other needs. Although this energy could be used to power
133 heat pumps leading to cooling capacity increase. Temperature of the liquid inside the ground
134 probes changed from -10°C at the inlet to -4°C at the outlet. Once calculated soil temperature
135 went below it, the heat pump was considered as switched off, i.e., α was zeroed. Ground probes
136 were placed at 20 cm depth with 20 cm between the axes of 25 mm outer diameter, 2 mm thick
137 wall polyethylene pipes.



138

139 Figure 2. Considered sites and their position regarding to permafrost and railroads



140

141 Figure 3. Calculation area and mesh characteristics: 1 – solar panels, 2 – ground probes, 3 – soil
 142 surface (number of cells – 48951; number of cells on the X axis – 441; number of cells on the Y
 143 axis – 1; number of cells on the Z axis – 111).

144

145 Table 1. Soil layers composition

Norilsk				Yakutsk				Chita			
Soil	Layer thickness, m	Moisture	Phase transition temperature, °C	Soil	Layer thickness, m	Moisture	Phase transition temperature, °C	Soil	Layer thickness, m	Moisture	Phase transition temperature, °C
Peat	0.5	3.47	0	Peat	0.3	3.47	-0.13	Sandy loam	2.3	0.1	-0.2
Clay loam	1	0.25	-0.21	Sand	1	0.4	-0.11	Sand	1.2	0.2	-0.12
Sandy loam	19	0.5	-0.16	Sandy loam	5	0.56	-0.16	Gravel	16.5	0.2	0
				Clay loam	14	0.66	-0.21				

146

147

148 Table 2. Climatic data for Norilsk

Month	Solar irradiation. kWh/(m ² *mon.), (averaged W/m ²)	Mean air temp., °C	Mean wind speed, m/s	Snow layer, cm	Soil temperature at depths, °C				
					20 cm	40 cm	80 cm	160 cm	320 cm
1	0.31 (0.4167)	-26.2	5.1	21.33	-4.1	-2.6	-1.7	-0.3	-1.1
2	8.68 (12.9167)	-24.2	4.8	21.00	-7.6	-5.4	-4.0	-0.6	-1.0
3	42.16 (56.67)	-19.2	4.3	21.67	-6.2	-4.8	-4.2	-1.4	-0.9
4	97.2 (135)	-14.4	4	21.33	-5.3	-4.6	-4.2	-2.1	-1.0
5	146.94 (197.5)	-5.3	3.7	12.67	-0.3	-2.2	-2.3	-2	-1.3
6	155.1 (215.4167)	4.1	3.6	0.00	0.1	-0.6	-0.9	-1.5	-1.5
7	152.83 (205.4167)	12.7	3.8	0.00	9.7	5.3	-0.1	-1.0	-1.4
8	102.61 (137.9167)	10	3.8	0.00	6.4	4.8	3.3	-0.4	-1.3
9	53.4 (74.167)	1.7	4	0.00	4.8	4.5	3.7	0	-1.3
10	19.53 (26.25)	-10.6	4.4	6.33	1.7	1.9	1.8	0.2	-1.0
11	1.8 (2.5)	-20.9	4.8	13.33	-0.9	-0.2	0	0	-1.0
12	0 (0)	-24.9	5	18.00	-7.8	-4.7	-1.9	-0.3	-1.0

149 Table 3. Climatic data for Yakutsk

Month	Solar irradiation. kWh/(m ² *mon.), (averaged W/m ²)	Mean air temp., °C	Mean wind speed, m/s	Snow layer, cm	Soil temperature at depths, °C				
					20 cm	40 cm	80 cm	160 cm	320 cm
1	8.06. (10.83)	-36.5	1.5	26.1	-7.4	-6.4	-3.7	-0.2	-0.6
2	22.68. (33.75)	-35.1	1.5	31.4	-8.5	-7.4	-5.3	-0.9	-0.5
3	86.18. (115.83)	-15.4	1.9	31.4	-6.9	-6.3	-4.9	-1.7	-0.5
4	134.1. (186.25)	-2.1	2.7	15.3	-4.3	-3.9	-3.3	-1.7	-0.5
5	163.37. (219.58)	9.5	3.5	0	4.0	1.7	-1.5	-1.3	-0.5
6	175.8. (244.17)	16.1	3.1	0	12.8	10.5	4.6	-0.9	-0.5
7	166.47. (223.75)	22.5	2.9	0	20.8	17.3	10.7	0.6	-0.5
8	132.06. (177.5)	17.4	2.8	0	15.4	14.6	12.3	5.2	-0.5
9	72.3. (100.42)	3.8	2.6	0	6.0	6.3	6.4	4.8	-0.5
10	37.82. (50.83)	-5.1	2.6	5.6	0.3	0.9	1.9	2.2	-0.3
11	12.6. (17.5)	-26.5	1.9	17.1	-2.5	-1.6	-0.6	0.3	-0.5
12	4.34. (5.83)	-36.1	1.5	23.4	-4.8	-3.4	-1.2	-0.2	-0.5

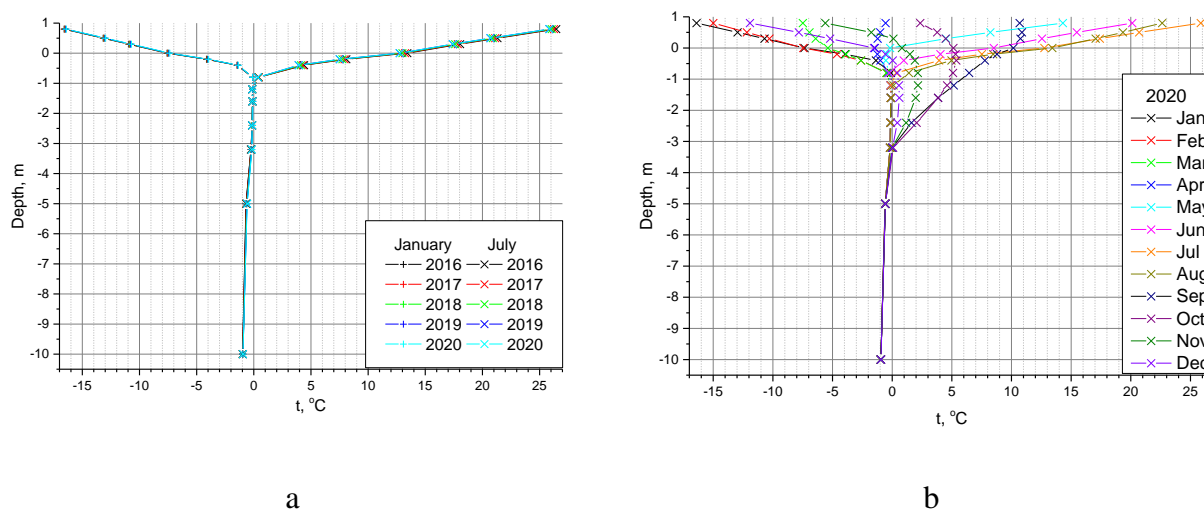
150 Table 4. Climatic data for Chita

Month	Solar irradiation. kWh/(m ² *mon.), (averaged W/m ²)	Mean air temp., °C	Mean wind speed, m/s	Snow layer, cm	Soil temperature at depths, °C				
					20 cm	40 cm	80 cm	160 cm	320 cm
1	33.48 (45)	-27.2	1.4	18.1	-16.4	-11.9	-7.7	-2.4	1.0
2	59.92 (89.167)	-17.9	1.8	13.1	-16.6	-13.2	-9.6	-4.9	0
3	112.84 (151.67)	-6.6	3	3.3	-6.2	-5.5	-5.3	-4.6	-0.4
4	145.8 (202.5)	4.8	4.1	0	5.2	2.7	-0.8	-1.8	-0.7
5	180.11 (242.083)	9.8	4	0	12.0	8.6	5.0	0.6	-0.2
6	184.2 (255.83)	18.6	3.1	0	20.9	15.9	10.6	4.5	0
7	165.23 (222.083)	19.1	2.6	0	19.6	17.7	14.0	8.4	3.1
8	138.57 (186.25)	18.3	2.3	0	17.7	17.1	15.4	11.2	6.0
9	105.9 (147.083)	7.3	2.8	0.6	9.1	11.2	11.8	10.8	7.4
10	73.16 (98.33)	1.8	3	0	6.6	6.9	7.3	7.9	7.0
11	39.3 (54.583)	-14.7	2.7	0.5	-10.1	-3.8	0.6	3.9	5.4
12	25.73 (34.583)	-23.4	1.8	4.0	-16.7	-11.5	-6.5	-0.3	3.0

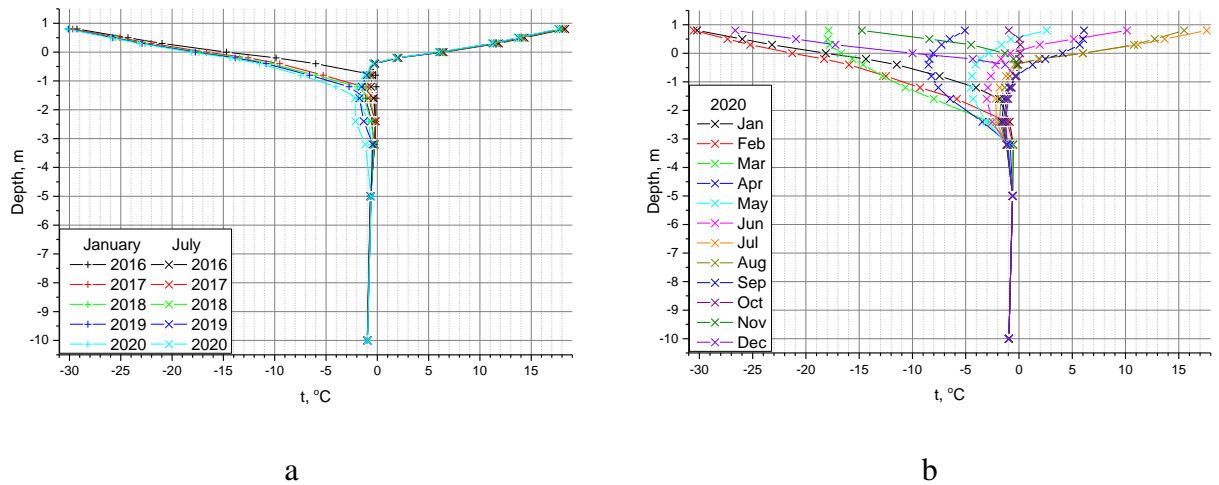
151 **4. Results**

152 *4.1. Verification of calculations and traditional methods*

153 Figure 4a shows the year-to-year stability of the soil temperature at natural conditions to
154 evaluate the stability of the calculation model. Figure 4b shows monthly distributions in 5 years
155 after calculation start. Those were in good agreement with the existing reference data (Table 3).
156 The next step was to evaluate solar panels shielding effect on the soil temperature distributions
157 (Figure 5). It can be seen that surface temperature becomes significantly lower due to no snow
158 cover under the shields. However, in-depth soil temperature is almost not affected. For this
159 reason, maximum surface temperature is also decreasing, but to lower extent, and thawing layer
160 is reduced by nearly 0.5 m. Solar blinds have been used at the Baikal-Amur railroad to the south
161 of Yakutsk; thawing layer was reduced from 4.0 m to 1.51 m in 5 years, correspondingly [27].
162 The effect of solar blinds is proportional to the radiation to convection heat flux ratio. For this
163 reason, strong effect has been shown for Tibet [14]. But in some cases, 1.5 m thawed layer is still
164 not appropriate.



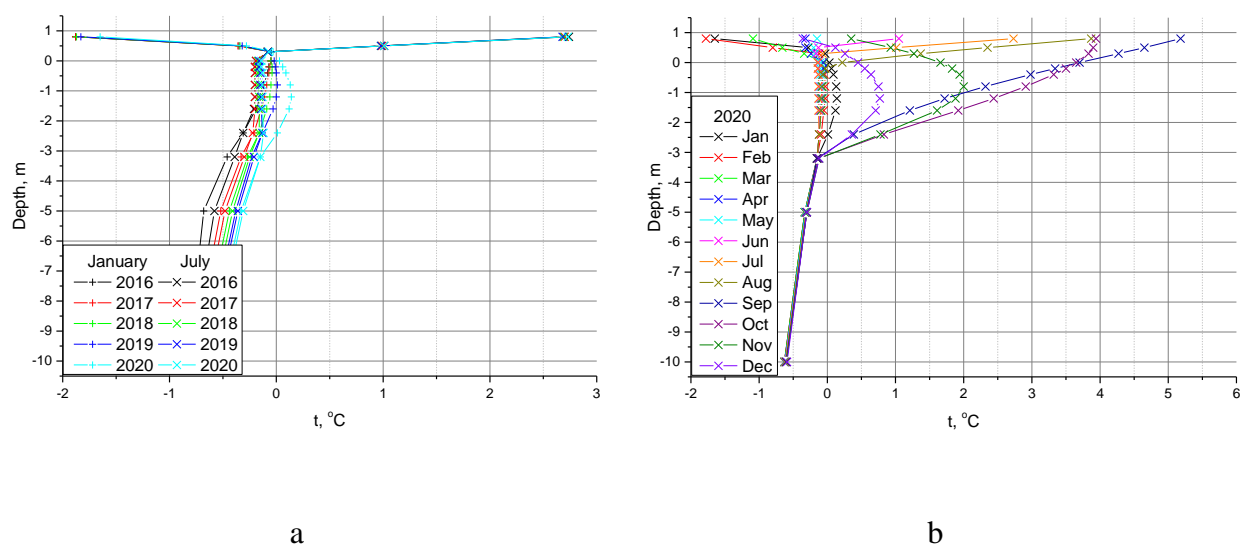
165 Figure 4. Calculated temperature distribution at natural conditions to check for basic equilibrium
166 in Yakutsk (a – July and January in 2016–2020; b – monthly distribution in 2020)



167 Figure 5. Temperature distribution under PV solar shields in Yakutsk (a, b – see Figure 4)

168

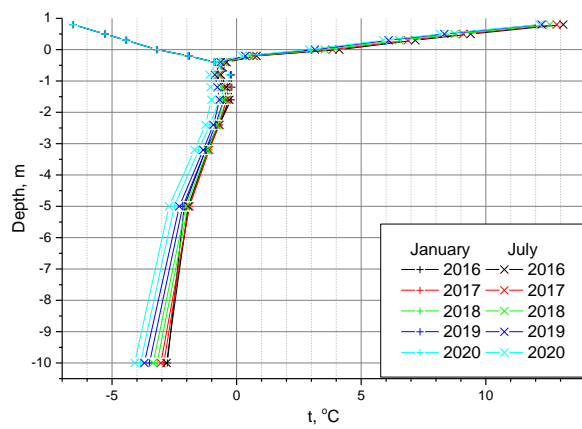
169 Another way for shielding soil from the external heat is covering with the heat insulation
 170 layer. Crushed rock is a more usual and universal one, but polystirol sheets are also used for this.
 171 We have considered such way for Chita (Figure 6) since summer heating is rather high there, and
 172 convective part should also be rejected to get small thawing layer. However, such heat insulation
 173 prevents intense freezing in winter. For deep snow regions, it gives low additional effect, but
 174 snow cover is thin in Chita (Table 4). As a result, cooling in winter is very poor and highest
 175 temperatures are reached in September/October due to thermal conduction from the unshielded
 176 areas. Even though a thawed layer of several meters is still present, it exists for shorter time and
 177 is still thinner than at natural conditions. Another feature of this case is positive long-term
 178 temperature drift caused by low cooling in winter (Figure 6a), while all other cases are showing
 179 neutral or negative trend. This case is also sensitive to the season when heat insulation is applied.
 180 If done in September, the soil is preserved in warm state and thawed deeper. If done in April, just
 181 after snow is gone, soil is preserved in the cooled state presented in Figure 6.



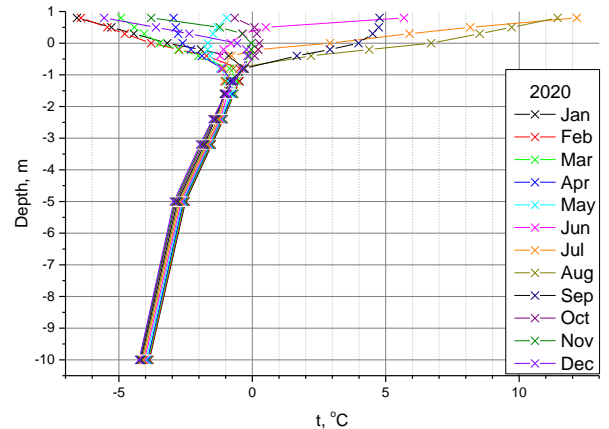
182 Figure 6. Temperature distribution under 50 mm polystyrol heat insulation in Chita (a, b – see
 183 Figure 4)

184

185 Thermosyphons widely used for permafrost thermal stabilization give a similar effect for
 186 the embankment axis (Figure 7) compared to the solar blinds (Figure 5). While the latter are
 187 covering the embankment slopes uniformly, the former are forming cool spots, and their effect is
 188 decreasing with distance. If the evaporator part is vertical, the embankment axis can be too far to
 189 see the cooling effect, while frozen walls preventing soil movement are still formed aside, and
 190 deep layers are gradually cooling down. To make the embankment core frozen, inclined
 191 evaporators are used, but this complicates the thermosyphon design, logistics, and installation.
 192 The soil is still thawing down to 1.5 – 2.0 m since it is heated in summer, but this layer stays for
 193 a shorter time than at natural conditions. The time gap between artificial cooling and natural
 194 heating leads to the present issues in the warming climate. E.g., in hot summer after a warm
 195 winter, thawed gaps in the thermosyphon rows appear leading to wet soil movement through
 196 those bottlenecks. Noteworthy, dry and rocky soils characteristic for the southern edge of the
 197 permafrost extent are even less capable of such cold accumulation.



a

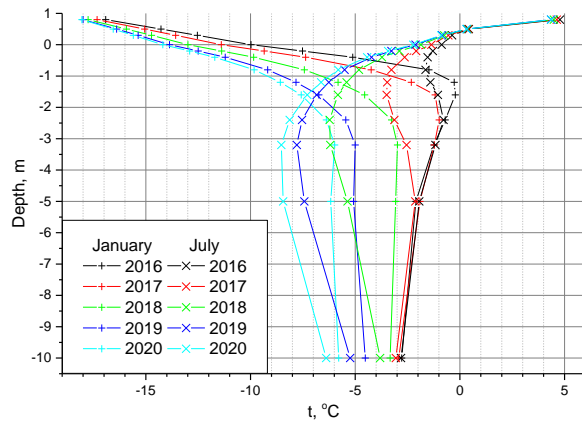


b

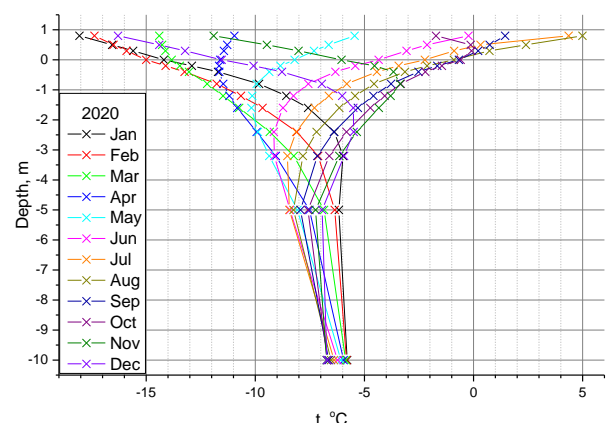
198 Figure 7. Temperature distribution under thermosyphons in Norilsk (a, b – see Figure 4)

199

200 To prevent this, the active cooling of thermosyphons is used in summer, solar powered
 201 chillers can be used to make such systems autonomous [18]. Or solar blinds could be combined
 202 with thermosyphons, but our calculations show (Figure 8) that despite certain effect in Norilsk,
 203 this way is still incapable of thawing layer prevention farther south. Neither does combination of
 204 heat insulation with solar panels since the latter do not add anything sufficient to the shielding
 205 effect.



a



b

206 Figure 8. Temperature distribution under solar blinds combined with thermosyphons in Norilsk

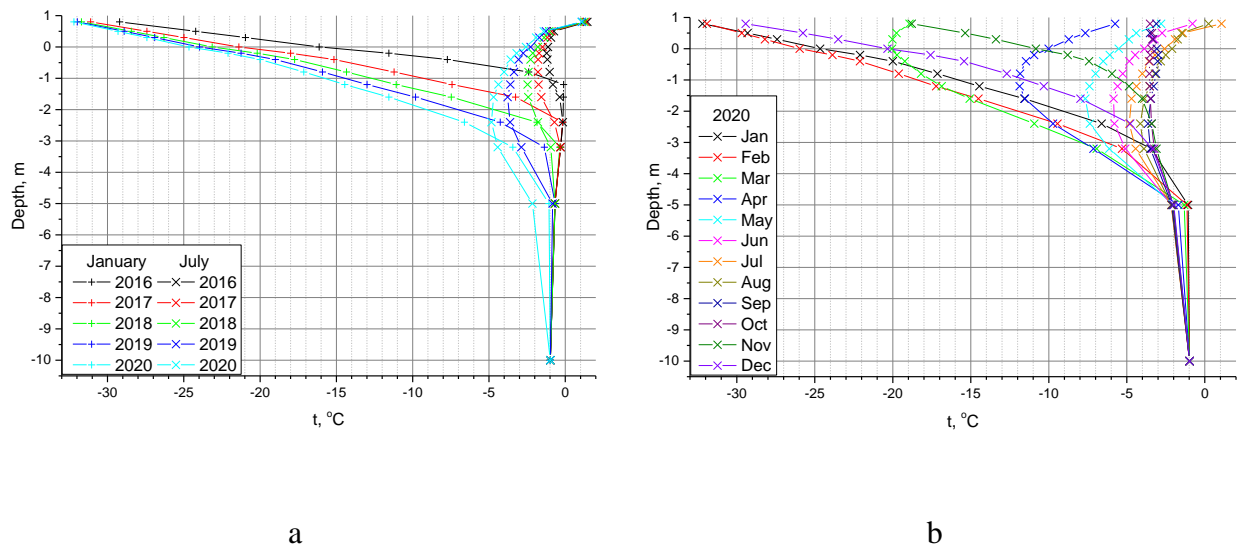
207 (a, b – see Figure 4)

208

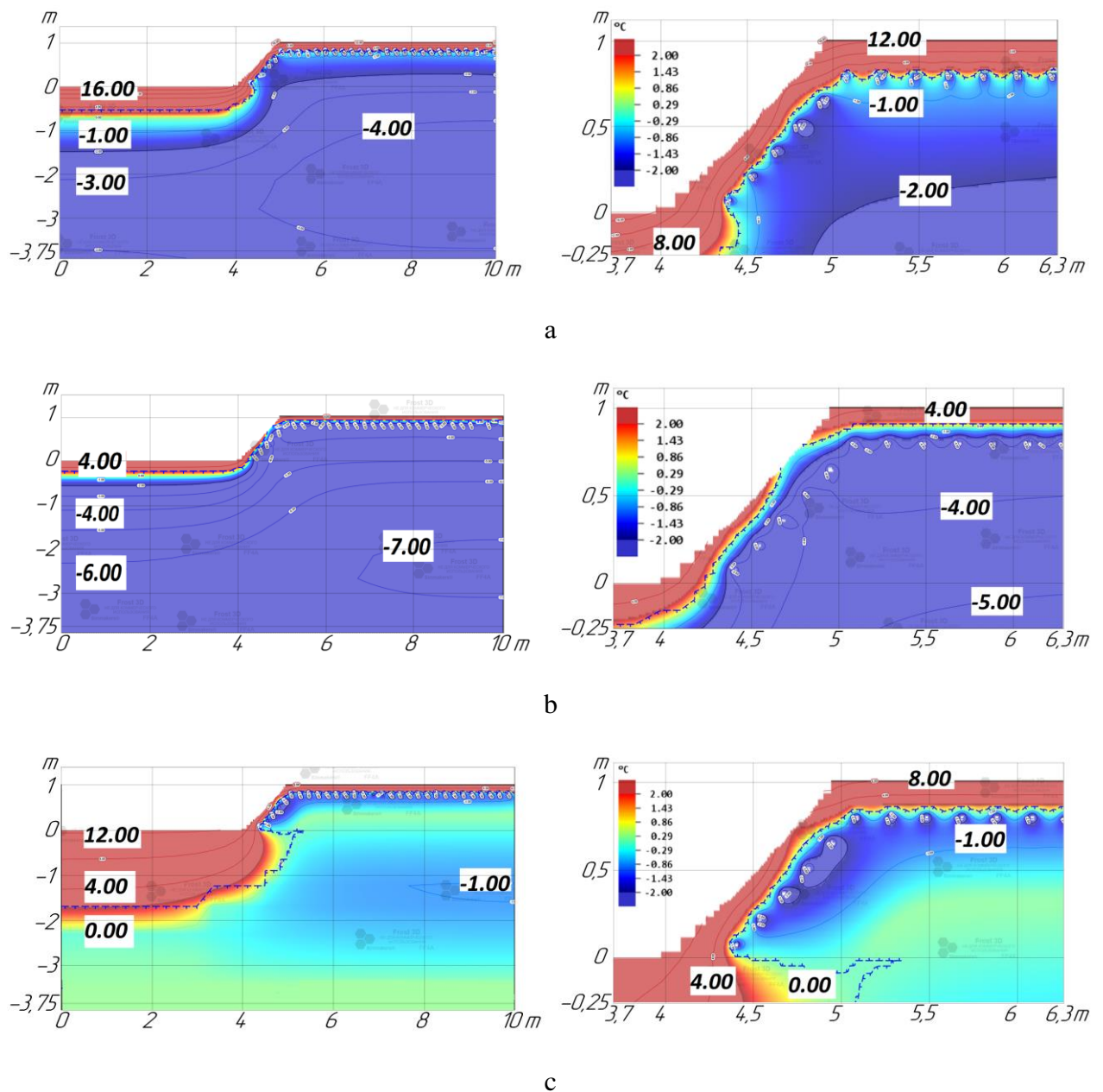
209

210 4.2. Implementation of the suggested approach

211 Our approach suggests that cooling should be applied in summer not to the deep layers
212 but to the soil surface – to prevent heat penetration completely. In terms of hardware, the system
213 should be some similar to the one described in [18], but ground probes should be placed
214 horizontally, like in floor heating, and solar panels (or at least blinds) should cover most of the
215 protected area. Figure 9 shows that almost no thawing layer is possible in Yakutsk conditions,
216 and there is remarkable negative temperature drift both in summer and winter even after 5 years
217 of system operation. Figure 10 indicates clearly that heat does not penetrate beyond the ground
218 probes even in the warmest conditions of considered, placing those closer to the surface can even
219 eliminate thawing layer completely as soon as heat source is balanced with heat sink. Figure 10c
220 is particularly interesting because the embankment stays frozen in summer while thawed layer is
221 formed in-depth aside by long-distance thermal conduction.



222 Figure 9. Temperature distribution under PV with near-surface ground probes in Yakutsk (a, b –
223 see Figure 4)

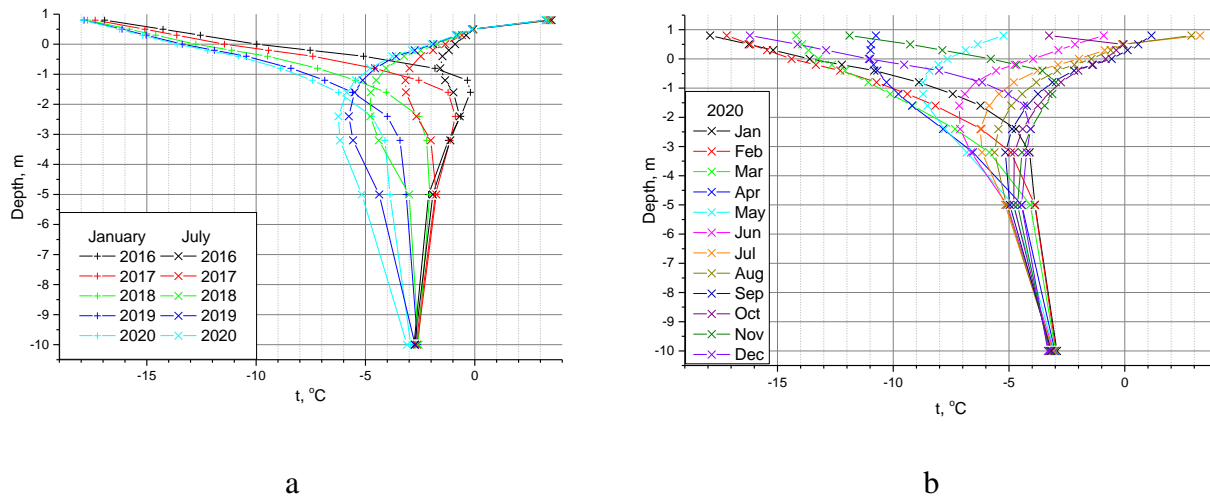


224 Figure 10. Temperature maps under PV with near-surface ground probes in July 2020 (a –
 225 Yakutsk, b – Norilsk, c – Chita; left – general view, right – magnified upper edge of the
 226 embankment)

227

228 There is a more exotic way to form a thermal shielding layer – spraying of the artificial
 229 snow under the solar panels. Although the application range for this way is more limited. Of
 230 considered sites, it worked in Norilsk only leading to thawing layer of less than 0.5 m (Figure
 231 11). This way is much more favorable for the alpine areas, where rocks and surface ice restrict
 232 using ground probes and convective heat flux is low. However, producing artificial snow

233 suggests intense supply of finely filtered water. We have evaluated 6 cm thick artificial snow
234 layer can be produced daily during months with positive mean air temperatures and based on this
235 performed calculations.



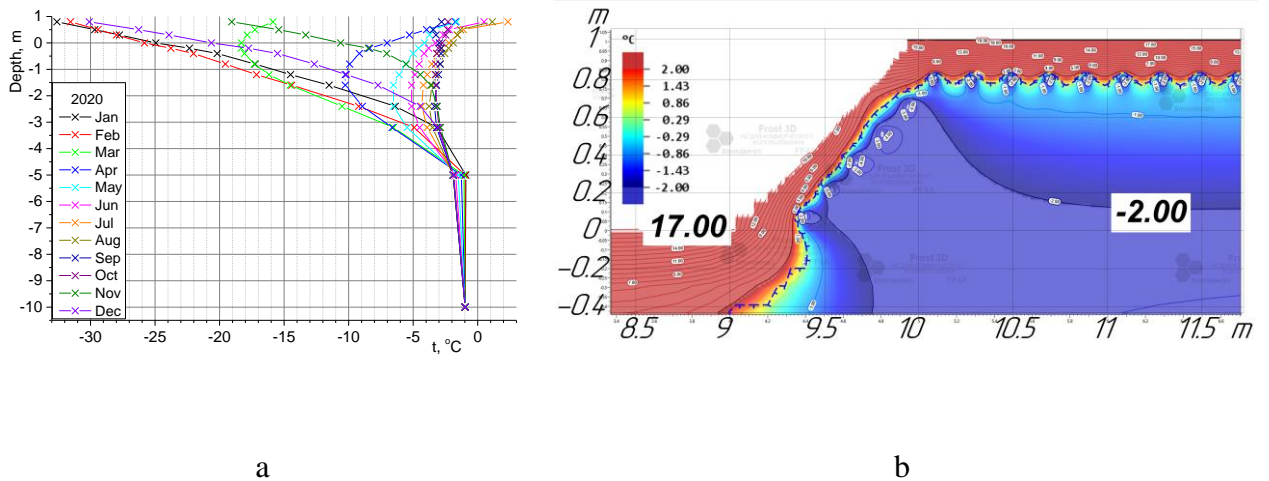
236 Figure 11. Temperature distribution under PV with 5 cm artificial snow layer in Norilsk (a, b –
237 see Figure 4)

238

239 5. Discussion

240 5.1. Application to real constructions

241 Even though sun elevation angles in the Arctic are low, we still suggest mounting solar
242 converters parallel to the ground surface to provide the best shielding and to reduce wind loads.
243 The exception relates to the fuel reservoirs, where vertical cylindrical surface is even more
244 desirable for solar panels (if safety regulations are matched). In case of insufficient power
245 supply, solar energy converters can cover the area bigger than what actually needs thermal
246 stabilization, except extra power, those provide a buffer layer of shielded soil that is still cooler
247 than at natural conditions. The example of such approach is presented in Figure 12. Without
248 shielding the top of the embankment, heat flux is higher than sinking to the ground probes, this
249 leads to deeper thawing. But side ground probes are forming frozen walls preventing thawed soil
250 tangential movement. Dull weather does not suggest strong heating, but additional use of wind
251 energy can be considered in certain cases.



253 Figure 12. Temperature distributions at realistic road embankment (paved with concrete, no PV
 254 atop of it) in Yakutsk with 1.8x cooling capacity due to use of power from extra solar panels
 255 outside the embankment.

256

257 Ideally, to reduce digging, ground probes are to be placed as close to the surface as
 258 possible. But, in this case, heat flow is maximized and, to provide a uniform temperature field,
 259 probes have to be close to each other. To some extent, this could be resolved by placing a heat
 260 insulation layer on top. But we suggest probes should be buried at 20 to 50 cm with about the
 261 same distance in between. Shallow horizontal ground probes are particularly useful in the
 262 regions with rocky general substrate, e.g., in the mountain areas. Thermal shielding layer could
 263 be particularly useful for saline soils since those are thawing deeper and need to be cooled to
 264 lower temperatures [28].

265 It has been shown that at permafrost thawing highest emission rates for CO_2 occur from
 266 0–40 cm depths, for CH_4 – from 40–80 cm [29]. High abundances of carbon-cycling bacteria,
 267 fungi, and archaea corresponded to 0–40 cm depths. Release of hazardous chemical, e.g.,
 268 mercury [30], has been reported too. So significant reduction of thawing layer and its
 269 temperature leads not only to better structure stability, but also prevents chemical and biological

270 hazards in the area of human activities. In critical cases, river and lake banks can be also shielded
271 using our approach to stop destruction and methane bubbling [31].

272 *5.2. Costs evaluation*

273 We have evaluated the basic cost of PV + vapor compression heat pump solution. PV
274 panels current spot price is 0.171 \$/W [32], and reasonable conversion efficiency for this price is
275 ca. 17% at STC, which gives 170 W/m² or 29 \$/m². PV panels represent ca. 40% of the solar
276 power plant cost, so 75 \$/m² can be assumed. This cost could be reduced if DC driven
277 compressors are used, so no invertors needed. Indeed, maximum power output for a horizontal
278 panel at N 60° latitude (maximum sun elevation angle 53.44°) will be reduced to ca. 100 W/m²,
279 so this value is to be used for available cooling capacity calculation. High COP vapor
280 compression pumps for a suitable temperature range cost ca. 1.0 \$/W_e, or 100 \$/m² (can be
281 reduced, see below). Usually, horizontal ground probes installation cost depends on excavation
282 works and is sufficient, but using cable laying machines in this case can reduce it to 2 \$/m²
283 including pipe. So the whole suggested thermal stabilization system cost starts at 177 \$/m².

284 Thermosyphon cost is ca. \$330 and it freezes area of ca. 3 m², its mounting costs at least
285 \$200, giving a total of at least 176 \$/m². For solar powered ground chillers [18], cost evaluation
286 by the authors is ca. 125 \$/m², but it is provided for system components only, not including
287 assembly and installation, which all can double the price. Of course, these cost evaluations are
288 coarse, but those show our solution might be economically competitive while providing cooling
289 exactly when it is needed and with positive feedback to solar radiation, resulting in nearly
290 guaranteed frozen state of the near surface soil layers. This feedback also resolves the problem of
291 faster thawing at southern slopes – at more intense solar flux.

292 The reduction of construction and maintenance costs at guaranteed permafrost thermal
293 stabilization needs special consideration. Rough estimates show that these savings are at least
294 half of the suggested solution cost, so making it eventually cheaper than traditional approaches.
295 In case energy pumped out of the ground is supplied for heating rather than released to the

296 atmosphere, additional income is generated. For example, ca. 0.3 Gcal/(m²*yr) output in Norilsk,
297 at local rates for heating reaching 235 \$/Gcal for isolated small communities [33], results in
298 saving up to 70 \$/(m²*yr). Even though half to quarter of this are more usual rates for
299 comparatively developed sites in that region (and tenth for the city), the suggested system could
300 be paid off just in this way during its lifetime.

301 *5.3. Possible optimization*

302 The electricity is the most universal form of energy to be used in devices, but
303 photovoltaic (and thermovoltaic to even greater extent) conversion efficiency is rather low if
304 cheaper products are considered. While electricity-driven refrigeration units provide the highest
305 COP. As for any system, cooperation of elements at certain conditions should be considered. For
306 example, we can consider PV combined with a vapor compression cooler or a vacuum tube
307 collector – with an absorption cooler. Commercial PV has realistic efficiency of 15%, and
308 vacuum tube solar collectors have 60%. A good vapor compression heat pump would give us
309 COP of 4.0 while absorption pump (uses mainly heat and needs electricity for circulation pumps,
310 fans and other service) – just 2.0.

311 Multiplication of performance for these two cases gives approximate overall use of solar
312 energy of 60% and 120%. This still does not mean the latter configuration is better. While
313 vacuum tube pipes convert direct solar radiation only, some PV (a-Si, CIGS) can deal well with
314 the diffused radiation too. In reverse, at higher ambient temperature, vacuum tube efficiency
315 grows while it goes down for PV (except some non-mass production materials). Vapor
316 compression coolers specific cost is lower than absorption ones at cooling capacity below
317 ca. 2 MW. COP of vapor compression heat pumps can be improved if piston compressors
318 (invertors) are powered with DC current from solar panels without double conversion
319 DC/AC/DC as in conventional grids. All this is to show a number of tradeoffs to be resolved in
320 each certain case.

321 At first glance, bulk energy storage (except minimum needed for control units operation
322 and slight damping of power supply intermittence) will not be paid off. Since in this case the soil
323 is the major and free storage of the demanded thermal energy. What could be optimized is PV to
324 cooling unit peak capacity ratio. Capacity factor for PV part depends a lot on local conditions,
325 and for horizontal panels is basically limited by the site latitude (on average, will not exceed
326 18%; in this case, it should be calculated for active season rather than the whole year). As it was
327 shown above, cooling unit specific price is significantly higher than PV, so its capacity factor is
328 worth optimization. For that, cooling unit operation should be uniform; could be supported by
329 driving energy storage. Bulk heat storage is considerably cheaper than electric, which gives
330 another advantage for solar thermal + absorption cooling configuration. But in case of excessive
331 electric energy generation, it could be sold out where applicable, so making investment in PV
332 power more cost effective than in energy storage.

333

334 **6. Conclusions and future work**

335 A sustainable way to reduce thawing layer depth to the first decimeters or eliminate it
336 completely is presented for the first time. The concept combines previously known ways of solar
337 radiation and precipitation shielding, solar powered cooling, and a novel approach suggesting
338 forming a near-surface thermal shielding layer. That is suggested to be formed by shallow
339 horizontal ground probes or, in some cases, by artificial snow. The cooling capacity of this
340 system has a positive feedback to the solar irradiation – the main component of soil heating.

341 In addition to infrastructure and buildings protection, this concept could be used to
342 prevent greenhouse gases release, and chemical and biological pollution from thawing
343 permafrost in the areas of human activities at least. We suggest this solution could be highly
344 demanded for constructions life cycle contracts; the evaluated cost of its implementation is
345 comparable to widely used thermosyphons while much better effect and further cost reduction
346 are expected.

347

348 **Acknowledgements**

349 We are grateful to Simmakers Ltd. for providing free remote access to the Frost 3D
350 package to ESS. Work of EYL has been supported by the Russian Ministry of Science and
351 Higher Education [state assignment No. 0705-2020-0046]. Equipment of the “Beam-M” facility
352 (Bauman Moscow State Technical University) has been used in this work. Authors are grateful
353 to J.P. Clements for English proofreading.

354

355 **References**

- 356 [1] O.A. Anisimov, Continental permafrost, Roshydromet, Moscow, 2012. doi.
357 [2] L. Chen, W. Yu, Y. Lu, W. Liu, Numerical simulation on the performance of thermosyphon
358 adopted to mitigate thaw settlement of embankment in sandy permafrost zone, Applied Thermal
359 Engineering, 128 (2018) 1624-1633. doi: <https://doi.org/10.1016/j.applthermaleng.2017.09.130>.
360 [3] E. Post, R.B. Alley, T.R. Christensen, M. Macias-Fauria, B.C. Forbes, M.N. Gooseff, A. Iler,
361 J.T. Kerby, K.L. Laidre, M.E. Mann, J. Olofsson, J.C. Stroeve, F. Ulmer, R.A. Virginia, M.
362 Wang, The polar regions in a 2°C warmer world, Science Advances, 5 (2019) eaaw9883. doi:
363 10.1126/sciadv.aaw9883.
364 [4] J. Van Huissteden, Thawing permafrost: Permafrost carbon in a warming arctic, 2020. doi:
365 10.1007/978-3-030-31379-1.
366 [5] A.V. Pavlov, G.F. Gravis, Permafrost and modern climate, Russian academy of science:
367 Priroda, 1016 (2000) 10-18. doi.
368 [6] C. Yuan, Q. Yu, Y. You, L. Guo, Deformation mechanism of an expressway embankment in
369 warm and high ice content permafrost regions, Applied Thermal Engineering, 121 (2017) 1032-
370 1039. doi: <https://doi.org/10.1016/j.applthermaleng.2017.04.128>.
371 [7] BBCNews, Arctic Circle oil spill: Russian prosecutors order checks at permafrost sites,
372 <https://www.bbc.com/news/world-europe-52941845>, accessed: 2020.09.17.
373 [8] C. Harvey, Can we refreeze the Arctic? Scientists are beginning to ask,
374 <https://www.eenews.net/stories/106007550>, accessed: 2020.09.17.
375 [9] S.W. Muller, H.M. French, F.E. Nelson, Frozen in time: Permafrost and engineering
376 problems, 2008. doi: 10.1061/9780784409893.
377 [10] G. Li, F. Wang, W. Ma, R. Fortier, Y. Mu, Z. Zhou, Y. Mao, Y. Cai, Field observations of
378 cooling performance of thermosyphons on permafrost under the China-Russia Crude Oil
379 Pipeline, Applied Thermal Engineering, 141 (2018) 688-696. doi:
380 <https://doi.org/10.1016/j.applthermaleng.2018.06.005>.
381 [11] D. Yinfei, W. Shengyue, W. Shuangjie, C. Jianbing, Cooling permafrost embankment by
382 enhancing oriented heat conduction in asphalt pavement, Applied Thermal Engineering, 103
383 (2016) 305-313. doi: <https://doi.org/10.1016/j.applthermaleng.2016.04.115>.
384 [12] J. Luo, F. Niu, M. Liu, Z. Lin, G. Yin, Field experimental study on long-term cooling and
385 deformation characteristics of crushed-rock revetment embankment at the Qinghai-Tibet
386 Railway, Applied Thermal Engineering, 139 (2018) 256-263. doi:
387 <https://doi.org/10.1016/j.applthermaleng.2018.04.138>.
388 [13] T. Wang, G. Zhou, D. Chao, L. Yin, Influence of hydration heat on stochastic thermal
389 regime of frozen soil foundation considering spatial variability of thermal parameters, Applied

390 Thermal Engineering, 142 (2018) 1-9. doi:
391 <https://doi.org/10.1016/j.applthermaleng.2018.06.069>.

392 [14] Y. Qin, Y. Li, T. Bao, An experimental study of reflective shading devices for cooling
393 roadbeds in permafrost regions, *Solar Energy*, 205 (2020) 135-141. doi:
394 <https://doi.org/10.1016/j.solener.2020.05.054>.

395 [15] C. Beer, N. Zimov, J. Olofsson, P. Porada, S. Zimov, Protection of Permafrost Soils from
396 Thawing by Increasing Herbivore Density, *Scientific Reports*, 10 (2020) 4170. doi:
397 [10.1038/s41598-020-60938-y](https://doi.org/10.1038/s41598-020-60938-y).

398 [16] I.M. Asanov, E.Y. Loktionov, Possible benefits from PV modules integration in railroad
399 linear structures, *Renewable Energy Focus*, 25 (2018) 1-3. doi: [10.1016/j.ref.2018.02.003](https://doi.org/10.1016/j.ref.2018.02.003).

400 [17] E.Y. Loktionov, E.S. Sharaborova, I.M. Asanov, Prospective Sites for Solar-Powered
401 Permafrost Stabilization Systems Integration in Russian Railways, in: 2019 8th International
402 Conference on Renewable Energy Research and Applications (ICRERA), IEEE, Brasov,
403 Romania, 2019, pp. 8996544.

404 [18] T.-f. Hu, J.-k. Liu, Z.-h. Hao, J. Chang, Design and experimental study of a solar
405 compression refrigeration apparatus (SCRA) for embankment engineering in permafrost regions,
406 *Transportation Geotechnics*, 22 (2020) 100311. doi: <https://doi.org/10.1016/j.trgeo.2019.100311>.

407 [19] H. Johra, K. Filonenko, P. Heiselberg, C. Veje, S. Dall'Olio, K. Engelbrecht, C. Bahl,
408 Integration of a magnetocaloric heat pump in an energy flexible residential building, *Renewable*
409 *Energy*, 136 (2019) 115-126. doi: <https://doi.org/10.1016/j.renene.2018.12.102>.

410 [20] U. Jakob, 6 - Solar cooling technologies, in: G. Stryi-Hipp (ed.) *Renewable Heating and*
411 *Cooling*, Woodhead Publishing, 2016, pp. 119-136. doi: [https://doi.org/10.1016/B978-1-78242-](https://doi.org/10.1016/B978-1-78242-213-6.00006-0)
412 [213-6.00006-0](https://doi.org/10.1016/B978-1-78242-213-6.00006-0).

413 [21] O.S. Popel, S.E. Frid, S.V. Kiselyova, Y.G. Kolomiets, N.V. Lisitskaya, Climate data for
414 renewable energy in Russia (Climatic database), MIPT Publishing, Moscow, 2010. doi:
415 [22] Research... Research and applications reference book on the climate of the USSR,
416 Hydrometeoizdat, Leningrad, 1989. doi:
417 [23] V.M. Veselov, I.R. Priblyskaya, Specialized arrays for climate research,
418 <http://aisori.meteo.ru/ClimateR>, accessed: 2020.11.18.

419 [24] V. Stolbovoi, I. McCallum, Land Resources of Russia,
420 http://webarchive.iiasa.ac.at/Research/FOR/russia_cd/copyright.htm, accessed: 2020.11.18.

421 [25] T.A. Dauzhenka, I.A. Gishkeluk, Consistency of the Douglas – Rachford splitting algorithm
422 for the sum of three nonlinear operators: application to the Stefan problem in permafrost soils,
423 *Applied and Computational Mathematics*, 2 (2013) 100-108. doi: [10.11648/j.acm.20130204.11](https://doi.org/10.11648/j.acm.20130204.11).

424 [26] A. Alekseev, G. Gribovskii, S. Vinogradova, Comparison of analytical solution of the semi-
425 infinite problem of soil freezing with numerical solutions in various simulation software, *IOP*
426 *Conference Series: Materials Science and Engineering*, 365 (2018) 042059. doi: [10.1088/1757-](https://doi.org/10.1088/1757-899x/365/4/042059)
427 [899x/365/4/042059](https://doi.org/10.1088/1757-899x/365/4/042059).

428 [27] V.G. Kondratyev, N.A. Valiev, Stabilization of soil at central part of Baikal-Amur railroad
429 using solar and precipitation blinds, in: International conference Kazakhstan-Cold, 1-2/03/2016,
430 Almaty, 2016, pp. 65-72.

431 [28] M. Angelopoulos, S. Westermann, P. Overduin, A. Faguet, V. Olenchenko, G. Grosse, M.N.
432 Grigoriev, Heat and Salt Flow in Subsea Permafrost Modeled with CryoGRID2, *Journal of*
433 *Geophysical Research: Earth Surface*, 124 (2019) 920-937. doi: [10.1029/2018jf004823](https://doi.org/10.1029/2018jf004823).

434 [29] L. Jiang, Y. Song, L. Sun, C. Song, X. Wang, X. Ma, C. Liu, J. Gao, Effects of warming on
435 carbon emission and microbial abundances across different soil depths of a peatland in the
436 permafrost region under anaerobic condition, *Applied Soil Ecology*, 156 (2020) 103712. doi:
437 <https://doi.org/10.1016/j.apsoil.2020.103712>.

438 [30] Z. Ci, F. Peng, X. Xue, X. Zhang, Permafrost Thaw Dominates Mercury Emission in
439 Tibetan Thermokarst Ponds, *Environmental Science & Technology*, 54 (2020) 5456-5466. doi:
440 [10.1021/acs.est.9b06712](https://doi.org/10.1021/acs.est.9b06712).

- 441 [31] K.M. Walter, S.A. Zimov, J.P. Chanton, D. Verbyla, F.S. Chapin, Methane bubbling from
442 Siberian thaw lakes as a positive feedback to climate warming, *Nature*, 443 (2006) 71-75. doi:
443 10.1038/nature05040.
- 444 [32] PVinsights, Solar PV Module Weekly Spot Price <http://pvinsights.com/>, accessed:
445 2020.09.17.
- 446 [33] Cost... Cost of thermal energy in Norilsk FY 2020, [https://stroyfora.ru/tariff/area-d301a980-](https://stroyfora.ru/tariff/area-d301a980-4a45-4066-9a20-4e783856a562/year-2020/type-9)
447 [4a45-4066-9a20-4e783856a562/year-2020/type-9](https://stroyfora.ru/tariff/area-d301a980-4a45-4066-9a20-4e783856a562/year-2020/type-9), accessed: 2020.12.03.
448
449